The mammalian Target of Rapamycin (mTOR) regulates T helper cell differentiation through the selective activation of mTORC1 and mTORC2 signaling

Greg M. Delgoffe, Kristen N. Pollizzi, Adam T. Waickman, Emily Heikamp, David J. Meyers, Maureen R. Horton, Bo Xiao, Paul F. Worley, and Jonathan D. Powell

Supplementary Figures 1-13

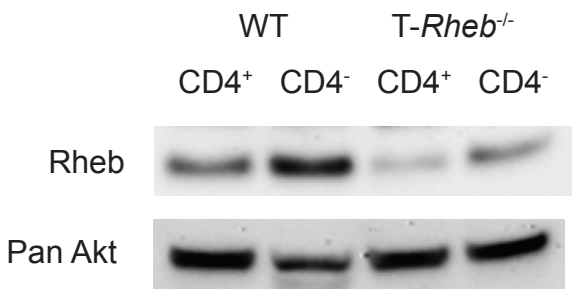

Supplementary Figure 1. Deletion of Rheb in T-*Rheb*$^{-/-}$ T cells. Immunoblot (IB) of lysates from wild-type and T-*Rheb*$^{-/-}$ CD4^{+} and CD4^{-} cells (which includes B cells, macrophages and dendritic cells) magnetically purified, lysed, and probed for Rheb1 protein. Akt is included as a loading control. Data are representative of three independent experiments.

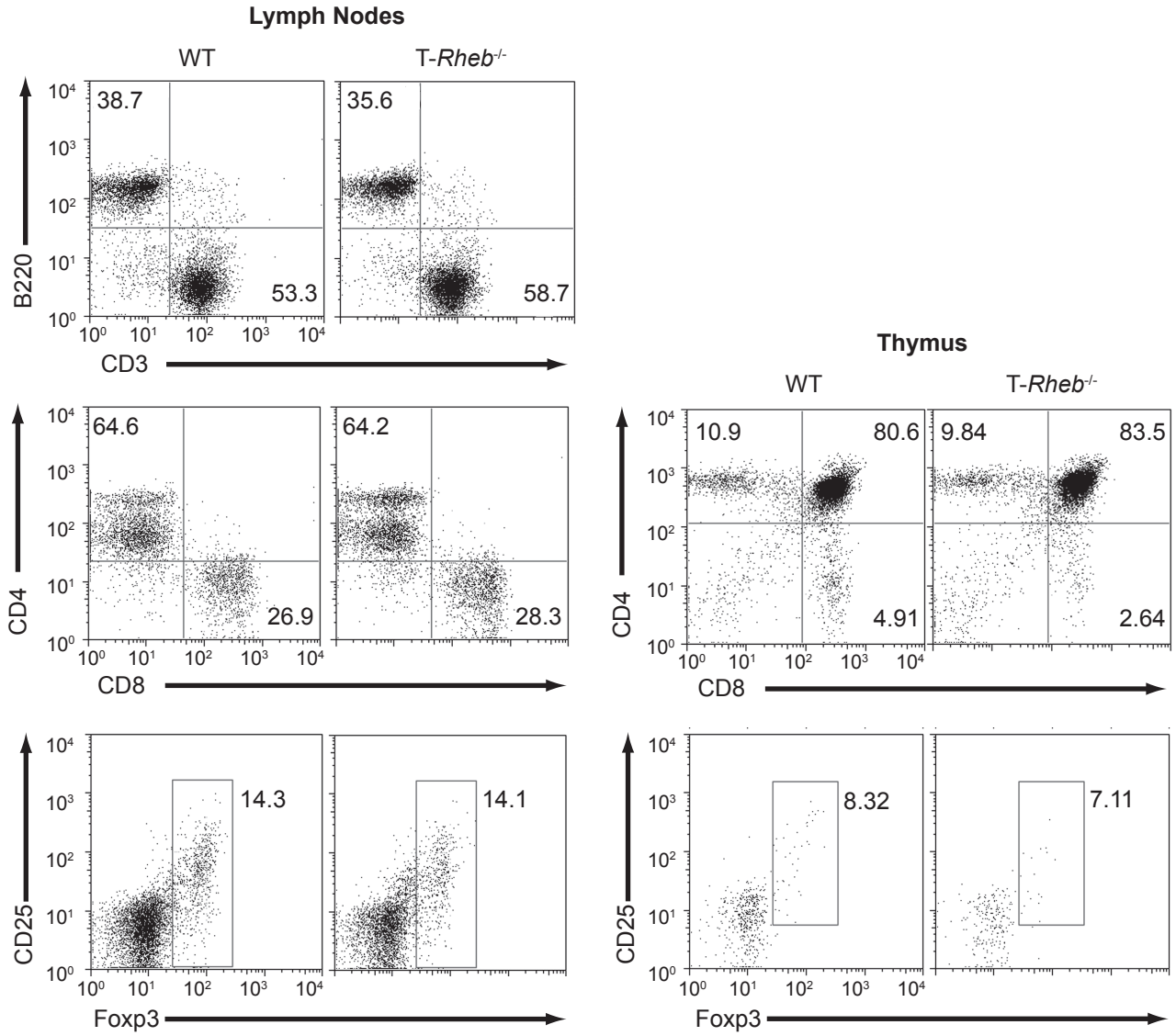

Supplementary Figure 2. Lymphoid development in T-*Rheb*$^{-/-}$ mice. Flow cytometric analysis of lymph node and thymic suspensions by flow cytometry. CD4 vs. CD8 plots are gated on CD3 cells. CD25 vs. Foxp3 plots are gated on CD4 cells. Data are representative of three independent experiments.

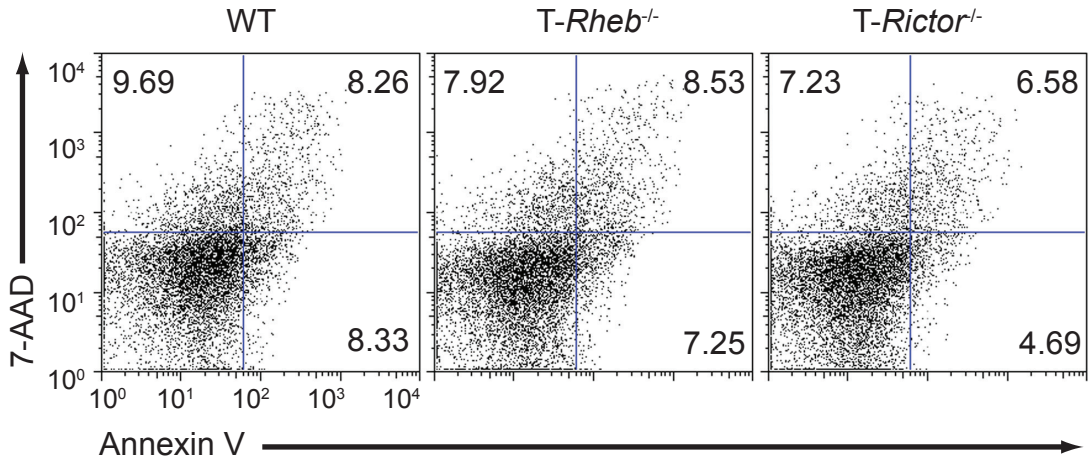

Supplementary Figure 3. No evidence of increased cell death in mTORC1 or mTORC2 knockouts. Apoptosis markers by flow cytometry of wild-type, T-*Rheb*$^{-/-}$, and T-*Rictor*$^{-/-}$ CD4^{+} T cells activated with anti-CD3 and APCs for 48 h. Plots are gated on CD3+CD4+ lymphocytes. Data are representative of three independent experiments.

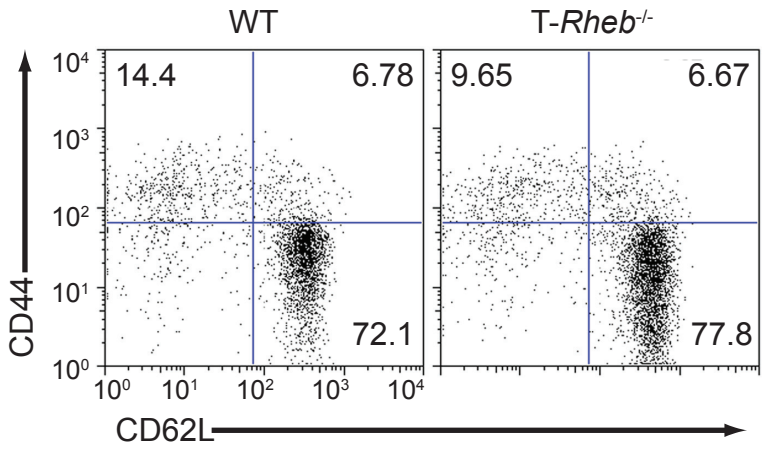

Supplementary Figure 4. Naive/effector memory ratios in T-*Rheb*$^{-/-}$ mice. Flow cytometric analysis of CD44 and CD62L expression of wild-type and T-*Rheb*$^{-/-}$ CD4^{+} T cells. Data are representative of three independent experiments.

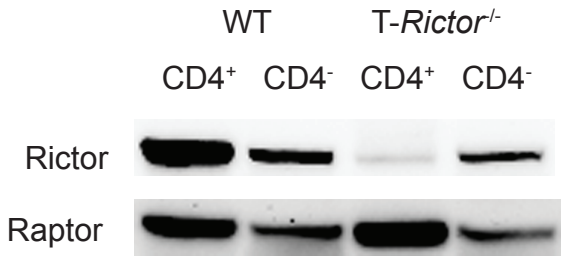

Supplementary Figure 5. Deletion of Rictor in T-*Rictor*$^{-/-}$ T cells. Immunoblot (IB) of lysates from wild-type and T-*Rictor*$^{-/-}$ CD4^{+} and CD4^{-} cells (which includes B cells, macrophages and dendritic cells) magnetically purified, lysed, and probed for Rictor protein. Raptor is included as a loading control. Data are representative of three independent experiments.

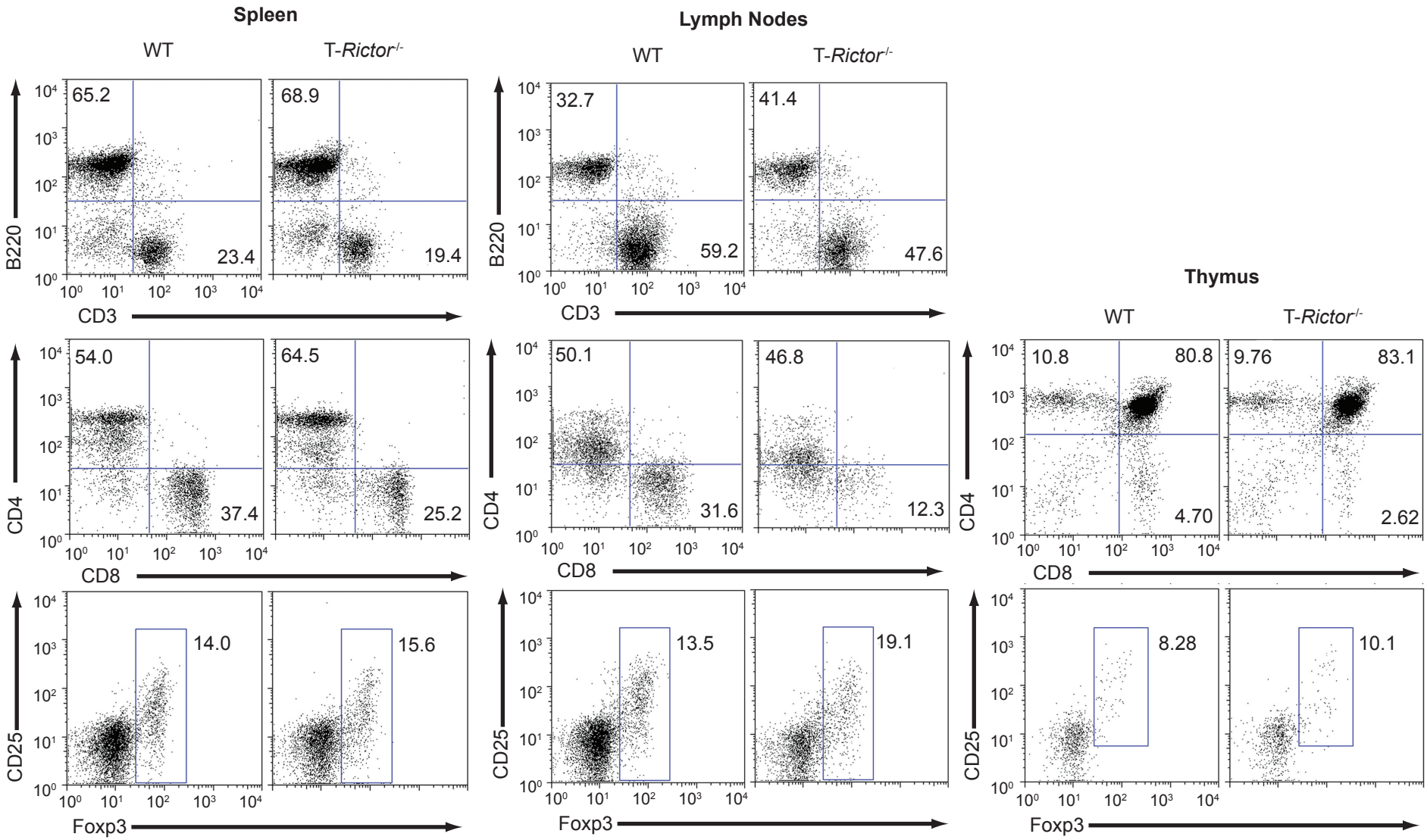

Supplementary Figure 6. Lymphoid development in T-*Rictor*$^{-/-}$ mice. Flow cytometric analysis of splenic, lymph node, and thymic suspensions by flow cytometry. CD4 vs. CD8 plots are gated on CD3 cells. CD25 vs. Foxp3 plots are gated on CD4 cells. Data are representative of three independent experiments.

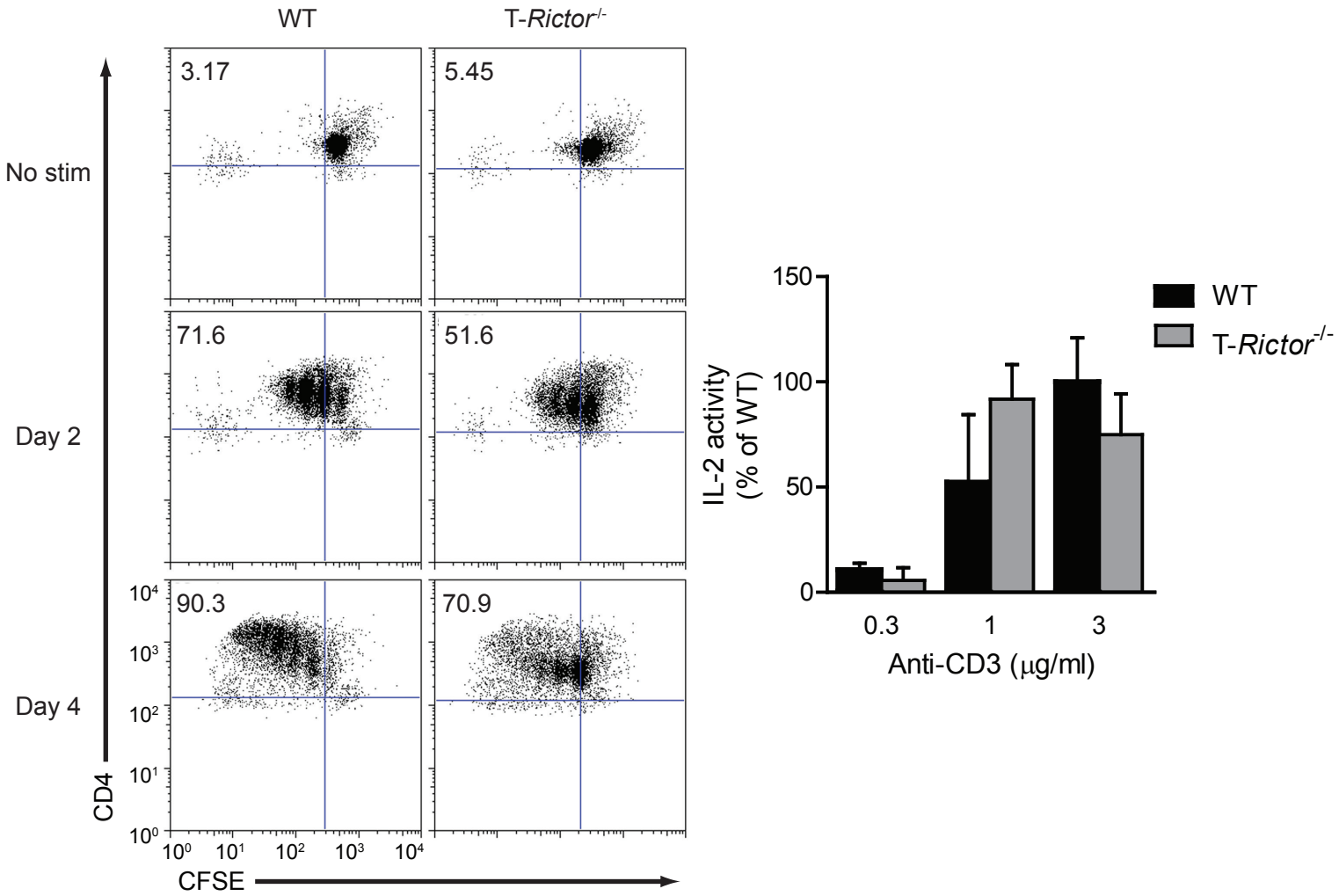

Supplementary Figure 7. Proliferation and T cell activation of Rictor-deficient T cells. CFSE dilution of wild-type and T-*Rictor*$^{-/-}$ CD4^{+} T cells labeled with CFSE and stimulated with anti-CD3 and APCs for the indicated times (left panel). IL-2 production of wild-type and T-*Rictor*$^{-/-}$ CD4^{+} T cells stimulated with anti-CD3 and anti-CD28 overnight. Data are representative of four independent experiments.

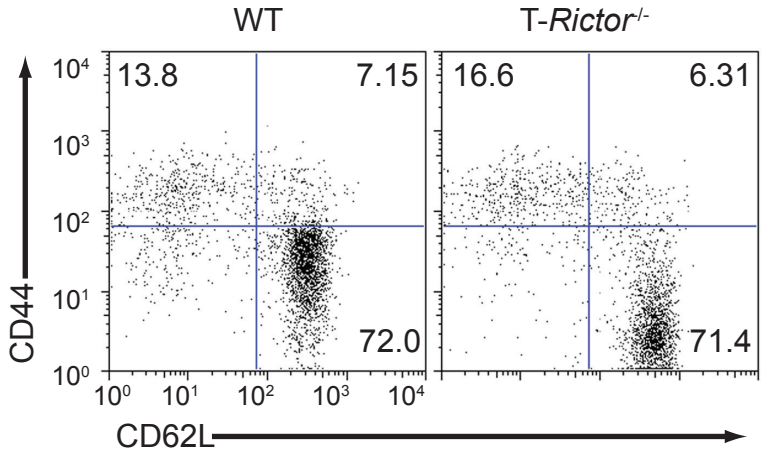

Supplementary Figure 8. Naive/effector memory ratios in T-*Rictor*$^{-/-}$ mice. Flow cytometric analysis of CD44 and CD62L expression of wild-type and T-*Rictor*$^{-/-}$ CD4^{+} T cells. Note the lower CD44 MFI seen in CD62L^{hi} T cells. Data are representative of three independent experiments.

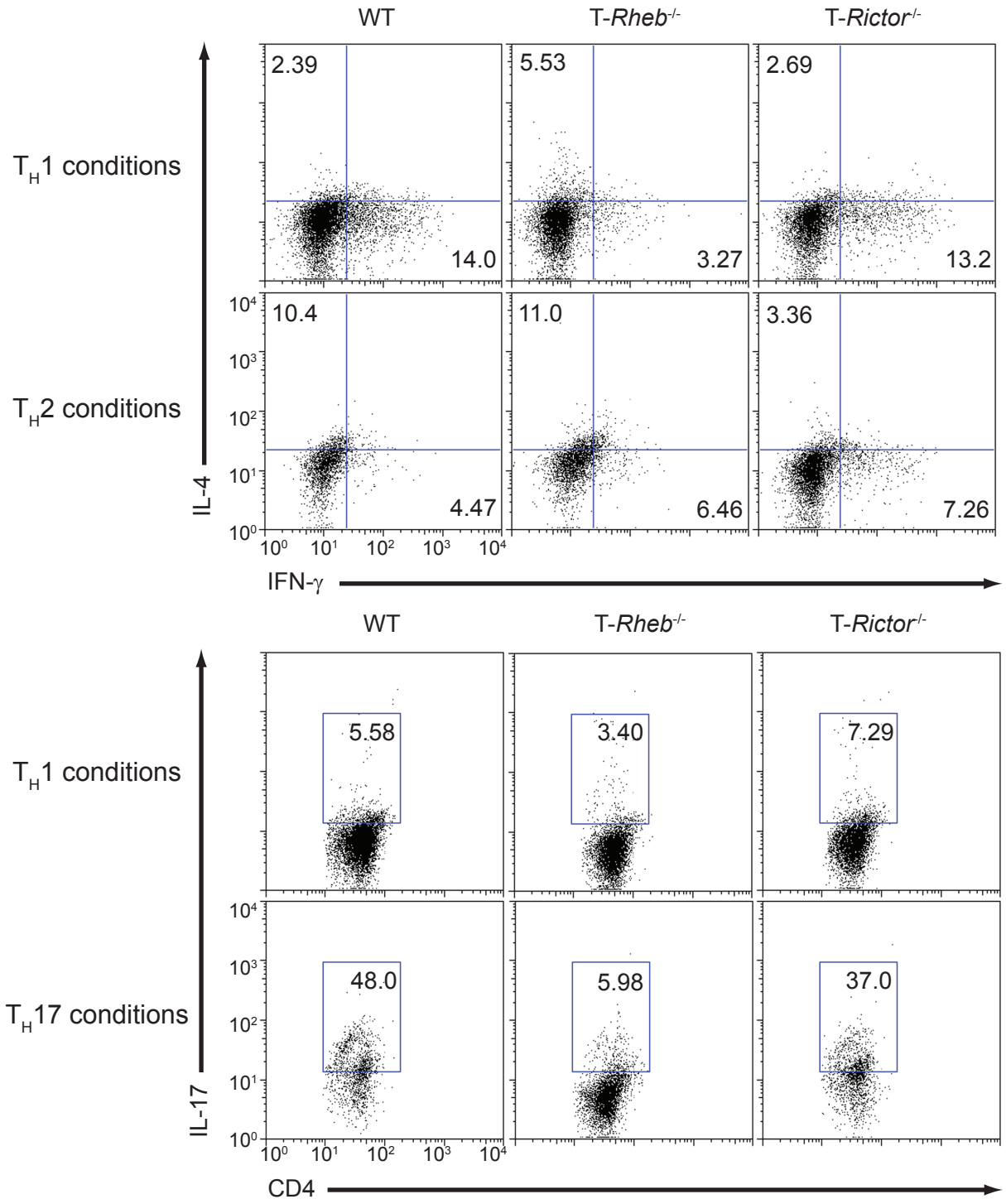

Supplementary Figure 9. Sorted naive T cells fail to skew similarly to bulk T cells. Cytokine production of wild-type, T-*Rheb*$^{-/-}$, and T-*Rictor*$^{-/-}$ CD4^{+} T cells sorted for CD4^{+}CD62L^{hi}CD44^{lo} naïve T cells (>98% purity). Cells were stimulated with anti-CD3 and anti-CD28 in skewing conditions, expanded in skewing conditions and IL-2 for 5 days, and restimulated with anti-CD3 and anti-CD28 overnight in the presence of a protein transport inhibitor. Data are representative of three independent experiments.

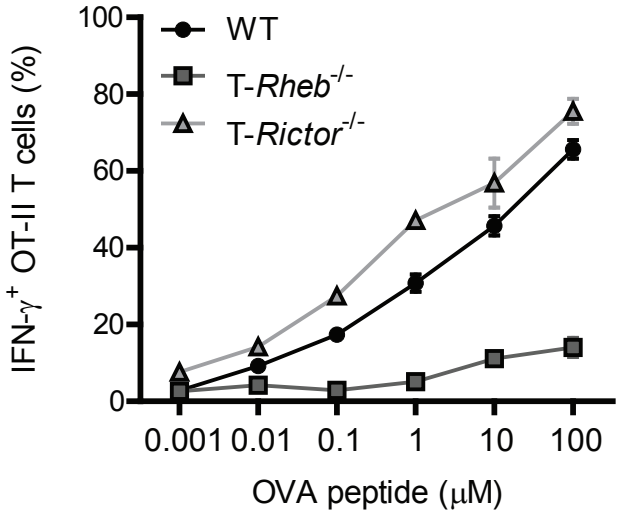

Supplementary Figure 10. Increased TCR signal strength does not rescue skewing in Rheb deficient cells. IFN-γ production of wild-type, T-*Rheb*$^{-/-}$, and T-*rictor*$^{-/-}$ CD4^{+} OT-II^{+} T cells stimulated *in vitro* with irradiated autologous APCs and varying doses of OVA peptide for 3 d, washed extensively, rested in IL-2 for 24 h, and restimulated with plate-bound anti-CD3 and anti-CD28 in the presence of a protein transport inhibitor. Results are plotted as percent IFN-γ^{+} by OVA peptide dose (μM) used for culture. Data are representative of two independent experiments.

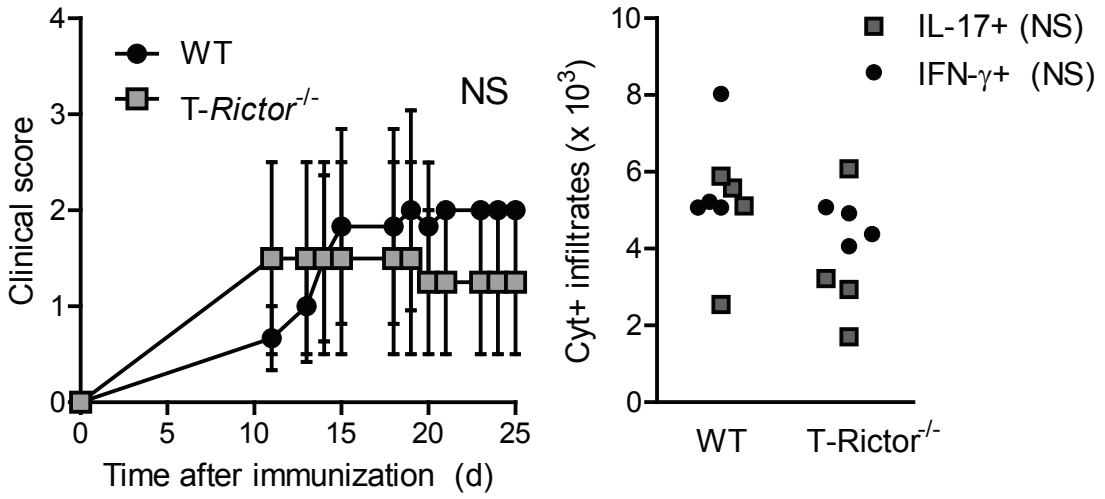

Supplementary Figure 11. Rictor-deficient T cells induce classical EAE. Disease progression for wild-type and T-*rictor*$^{-/-}$ mice immunized with MOG and CFA as previously described to induce EAE (left panel, n=4 mice, n.s. by one-way ANOVA). Cytokine production of CNS infilates isolated at the height of disease and stimulated with PMA and ionomycin (right panel, n=4, n.s. by Student's t test). Data are representative of three independent experiments.

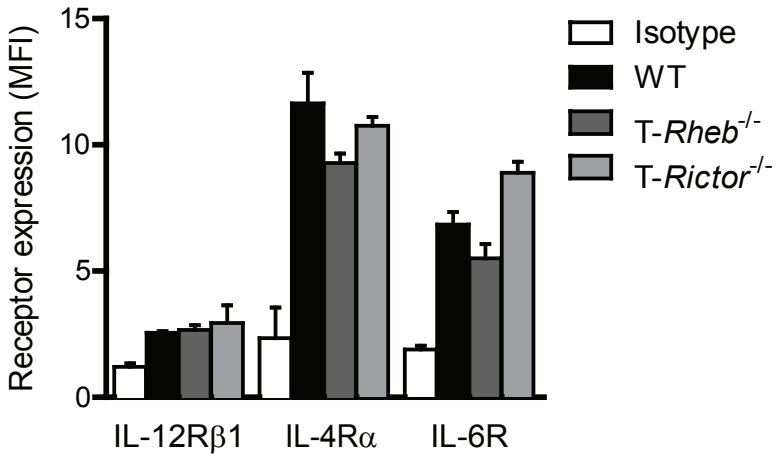

Supplementary Figure 12. Cytokine receptors are expressed normally in Rheb- and Rictor-deficient T cells. Expression of CD212 (IL-12Rβ1), CD124 (IL-4Rα), and CD126 (IL-6R) in wild-type, T-*Rheb*$^{-/-}$, and T-*rictor*$^{-/-}$ CD4^{+} T cells as measured by flow cytometry. Results are shown as mean fluorescence. Error bars indicate s.e.m. Results are pooled from three experiments.

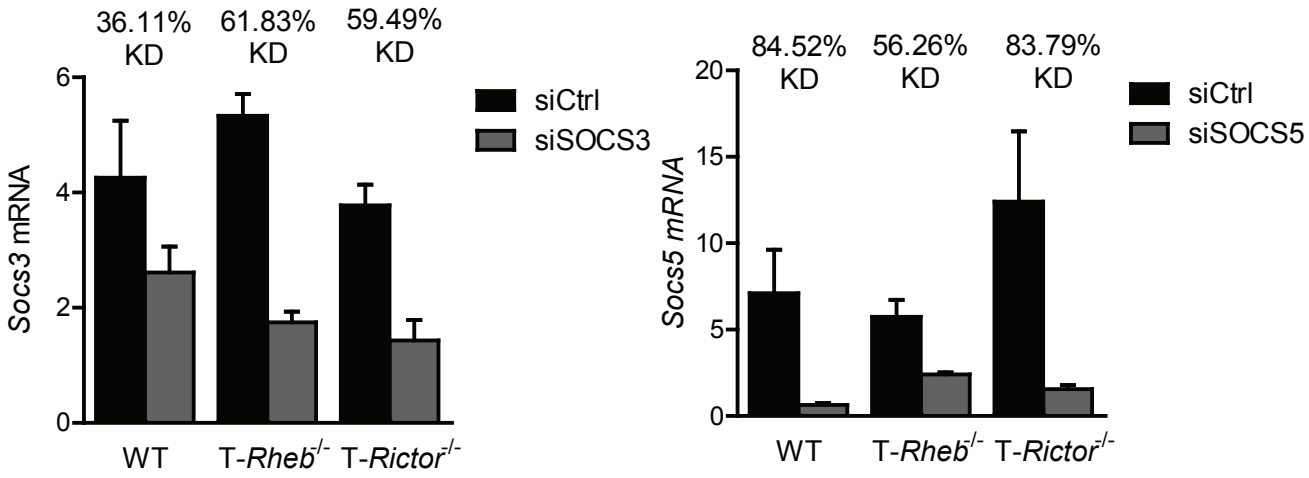

Supplementary Figure 13. siRNA knockdown efficiency of SOCS3 and SOCS5. SOCS3 and SOCS5 mRNA expression in wild-type, T-*Rheb*$^{-/-}$, and T-*rictor*$^{-/-}$ CD4^{+} T cells nucleofected with siRNA pools to scrambled (siCtrl), SOCS3, or SOCS5 by Amaxa nucleofection. RNA was extracted 16 hours after transfection. Knockdown was calculated by comparing to control-transfected cells. Results are representative of two independent experiments.